A 3-D SURFACE IMAGING LIDAR FOR MAPPING MARS AND OTHER BODIES FROM ORBIT

J. B. Abshire[1,2], X. Sun[1], E. Mazarico[1], J. W. Head III[3]; A. W. Yu[1], J.D. Beck[4]; [1] NASA Goddard Space Flight Center; [2]Univ. of Maryland College Park, [3]Brown University, [4]DRS Technologies, Dallas, Texas

Introduction: Space lidar measurements have made significant contributions to geophysics, geology, and other areas in planetary science. Lidar have been used in space for vertical profile measurements of surface and atmosphere over the past 20 years [1]. A major strength of laser altimetry (lidar measurements of surface elevation) is its geodetic accuracy, which allows planetary shapes to be determined so well as to enable placing constraints on internal structure and planetary evolution [2]. Early space lidars, such as the Mars Orbiter Laser Altimeter (MOLA) [3,4] and the Mercury Laser Altimeter (MLA) [5], used a single laser beam for measuring the surface elevation from orbit via the time-of-flight of the laser pulse. Five laser beams were used by the Lunar Orbiter Laser Altimeter (LOLA) to measure the lunar surface with higher spatial resolution and coverage [6].

Due to the small number of laser beams, the footprints of previous orbital lidar have not been contiguous and have sampled only a small fraction of the surface of the planetary bodies. Denser contiguous coverage of the surface with higher vertical resolution is required to address many important questions [7], particularly those for the Mars polar regions [8].

Developing a 3-D surface imaging lidar: Our team is developing a new 3-D imaging lidar to allow mapping Mars from orbit with contiguous 30-m pixels. The lidar utilizes new laser and detector technologies to enable measurements with ~60 laser beams in parallel in a 1.8 km wide cross-track swath. The 3-year activity started in summer 2018 and is supported by NASA's PICASSO program.

Figure 1 shows a comparison of single beam lidar measurements, such as MOLA, compared to a 3-D imaging lidar enabled by the new approach. With 30-m pixel resolution, global coverage of Mars can be achieved in about two years, allowing 3-D surface imaging with ~ 10 cm precision and meter-level geodetic accuracy.

This approach will enable global studies of Mars topography at much higher spatial and vertical resolution than is currently available. The lidar's 1.8 km swath and contiguous footprints allow complete planetary coverage during a typical mission, particularly in the polar regions, and will allow searches for surface changes with high spatial and vertical resolution at seasonal timescales.

This new 3-D imaging lidar can measure additional parameters along with the surface elevation. These include footprint-scale roughness from the return laser pulse shape, zero-phase surface reflectance from the return laser pulse energy [9], and regular (non-zero phase) surface reflectance from passive solar illumination. The lidar can also acquire height-resolved atmosphere backscatter profiles [10] to allow studies of atmosphere-surface interactions. Measurements of the distribution of aerosols and ice helps address key needs for Mars identified by the Mars Exploration Program Analysis Group.

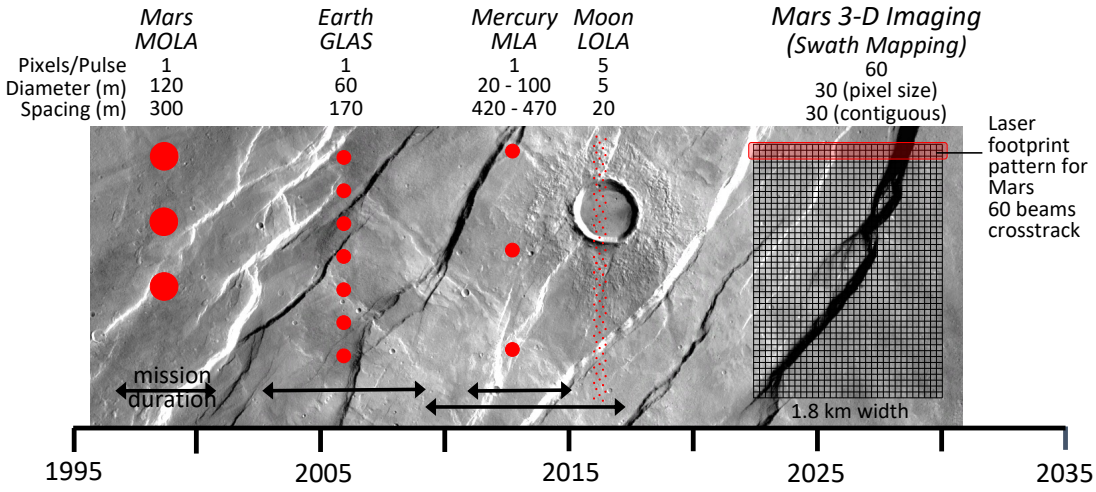

Figure 1 – *(Left to Right)* Illustration of the evolution of laser sampling of planetary surfaces from some previous orbital lidar overlayed on an image of the Mars surface. The right most image shows the sampling from this 3-D imaging lidar for Mars, that has contiguous surface sampling with ~30-m diameter footprints and ~10-cm vertical resolution.

Lidar Approach: This lidar approach is based on using more efficient lasers that emit shorter pulses at much higher rates, a 50-cm diameter receiver telescope and highly sensitive array detectors.

Laser - There are several candidate lasers that can meet our needs. For 3-D imaging lidar, the laser needs to have sufficient pulse energy to ensure a detectable signal for all pixels, emit short (nsec) pulse widths at kHz rates to reduce range error and provide contiguous coverage of the lidar ground track.

Our team previously developed such a laser under work supported by the ESTO Instrument Incubator Program [11]. It uses a master-oscillator power-amplifier (MOPA) design. The master oscillator is a passively Q-switched microchip Yb:YAG laser that emits nsec-wide pulses at 1030 nm. Its output energy is increased by a single-pass planar waveguide amplifier [12]. The prototype laser emits ~ 1.5 mJ per pulse at 7 kHz pulse rate. Our plan is to use this laser to illuminate a 60-footprint area with ~25 μJ /pixel per laser firing. Each 30-m ground footprint is sampled by ~70 laser pulses. The wall plug efficiency of this laser is ~11%, which is approximately twice that of previous flight lasers that were based on Nd:YAG.

Receiver Detector - We are developing a new highly sensitive array detector as the key receiver component to enable 3-D imaging lidar. The detector is a mercury-cadmium-telluride (HgCdTe) avalanche photodiode (APD) developed by DRS Technologies [13]. Array versions of this detector have been recently been developed and demonstrated and have a linear response. HgCdTe APD detectors have been developed over the past decade [14] and have a high (> 500) internal photoelectron multiplication gain, an analog response and nsec response times [15].

These detectors have demonstrated > 70% photon detection efficiency with linear response from 400 to 4300 nm [10]. Our team has previously developed a 2x8 pixel HgCdTe APD detector within a tactical cryo-cooler for the NASA Earth Science Technology Office (ESTO) Advanced Component Technology (ACT) program and the NASA InVEST program [16].

The combination of high speed, low dark noise and nearly noiseless gain has made HgCdTe APD detectors attractive for ground-based and airborne lidar. Due to their performance, integrated electronics, parallel pixel outputs and rugged packaging they are also well suited for use in space.

The individual pixel outputs from the detector array may also be separately summed to allow combining the detected signals from all laser beams. This is a substantial benefit when the return signal is weak and distributed in time, as it is from atmospheric backscatter. This approach allows this lidar instrument to also obtain vertically-resolved profiles of atmospheric backscatter simultaneously with surface mapping. These vertically resolved profiles will improve our understanding of the atmospheric processes through the 3-D mapping of dust, ice and clouds over the entire planet in both sunlight and darkness.

Ongoing work: Our team's ongoing work includes: completing an initial lidar design; further evaluating the Yb:YAG laser; developing the optical coupling approach for the lidar receiver; fabricating the 2x30 pixel HgCdTe APD array detector; characterizing its performance, and developing altimetry footprint analysis algorithms to reduce the data rate.

Once completed the results should enable further development of this type of lidar for mapping measurements from Mars orbit. Smaller versions of the lidar may also be used for measurements of other planetary bodies. Examples include mapping the topography of airless bodies such as asteroids and comet cores, tracking surface volatiles, and measuring the shapes and characteristics of plumes from icy moons.

References:

[1] Sun, X. et al. (2013) *IEEE Sel. Topics Appl. Earth Obs. Rem. Sensing*, 6, 1660. [2] Glaser, P. et al. (2013) *Planetary and Space Sci.,* 89, pp. 111. [3] M. T. Zuber, M.T. et al. (1992) *J. Geophys. Res*., 97, 7781. [4] Smith, D.E. et al. (2001) *J. Geoph. Res.*, 106, pp. 23689. [5] Zuber, M.T. et al., (2012) *Science*, 336, 217. [6] Smith, D.E. et al. (2010) *Space Sci. Rev.*, 150, 209. [7] Paige, D. A. (2017) *Lunar and Planetary Science (LPSC) XLVIII*, Paper 2633. [8] Byrne, S. (2009) *Annual Review of Earth and Planetary Sciences*, 37, 535. [9] Lucey, P. et al (2014) *J. Geophys. Res. Planets,* 119, 1665. [10] Neumann, G.A. et al. (2003) *J. Geophy. Res.: Planets*, 108, 5023. [11] Yu, A.W. et al. (2013) *Proc. SPIE* 8599, Paper 85990P. [12] Yu, A.W. et al. (2012) *CLEO* Technical Digest, paper JTh1I.6. [13] J. Beck, J. et al (2006) *J. Electron. Mater*., 6, 1166. [14] J. Beck, J. et al. (2014) *J. Electron. Mater.*, 43, 2970. [15] W. Sullivan W. III, et al. (2015) *J. Electron. Mater.*, 44, 3092. [16] X. Sun, X. et al. (2017) *Opt. Expr.*, 25, 16589.